1
т

Integrative analysis of transcriptomic and clinical data uncovers the tumor suppressive activity of MITF in prostate cancer

		۱	
-	,	,	

Lorea Valcarcel-Jimenez¹, Alice Macchia¹, Natalia Martín-Martín^{1, 2}, Ana Rosa Cortazar^{1, 2},
Ariane Schaub-Clerigué¹, Mikel Pujana-Vaquerizo¹, Sonia Fernández-Ruiz¹, Isabel LacasaViscasillas³, Aida Santos-Martin³, Ana Loizaga-Iriarte³, Miguel Unda-Urzaiz³, Ivana
Hermanova¹, Ianire Astobiza¹, Mariona Graupera⁴, Julia Starkova ⁵, James Sutherland¹, Rosa
Barrio¹, Ana M. Aransay^{1, 6}, Arkaitz Carracedo^{1, 2, 7,8} and Verónica Torrano^{1, 2, 9}

- 11 ¹CIC bioGUNE, Bizkaia Technology Park, 801^a bld., 48160 Derio, Bizkaia, Spain.
- 12 ²CIBERONC.
- 13 ³Department of Urology, Basurto University Hospital, 48013 Bilbao, Spain
- 14 ⁴Vascular Signalling Laboratory, Institut d´Investigació Biomèdica de Bellvitge (IDIBELL), Gran Via de l'Hospitalet 199-203.
- 15 ⁵CLIP-Childhood Leukaemia Investigation Prague, Charles University, Prague, Czech Republic; Second Faculty of Medicine,
- 16 Charles University, Prague, Czech Republic; University Hospital Motol, Prague, Czech Republic.
- 17 ⁶Centro de Investigación Biomédica en Red de Enfermedades Hepáticas y Digestivas (CIBERehd).
- 18 ⁷Ikerbasque, Basque foundation for science, 48011 Bilbao, Spain.
- ⁸Biochemistry and Molecular Biology Department, University of the Basque Country (UPV/EHU), P. O. Box 644, E-48080
 Bilbao, Spain.
- ⁹Correspondence to: Verónica Torrano, <u>vtorrano@cicbiogune.es</u>. Telephone number: 0034-944061326. Fax number: 0034944061301
- 23
- 24 The authors declare no conflict of interest.

25 **Abstract**

26 The dysregulation of gene expression is an enabling hallmark of cancer. Computational analysis of transcriptomics data from human cancer specimens, complemented with exhaustive clinical annotation, 27 28 provides an opportunity to identify core regulators of the tumorigenic process. Here we exploit well-29 annotated clinical datasets of prostate cancer for the discovery of transcriptional regulators relevant to prostate cancer. Following this rationale, we identify Microphthalmia-associated transcription factor 30 31 (MITF) as a prostate tumor suppressor among a subset of transcription factors. Importantly, we further 32 interrogate transcriptomics and clinical data to refine MITF perturbation-based empirical assays and unveil Crystallin Alpha B (CRYAB) as an unprecedented direct target of the transcription factor that is, 33 at least in part, responsible for its tumor suppressive activity in prostate cancer. This evidence was 34 supported by the enhanced prognostic potential of a signature based on the concomitant alteration of 35 36 MITF and CRYAB in prostate cancer patients. In sum, our study provides proof-of-concept evidence of the potential of the bioinformatics screen of publicly available cancer patient databases as discovery 37 platforms, and demonstrates that the MITF-CRYAB axis controls prostate cancer biology. 38

40 Introduction

Balanced integration of intracellular circuits operates within a normal cell to sustain physiological homeostasis. Alterations in some, if not all, of these circuits converge in changes on gene expression, which will eventually enable the acquisition and sustenance of the hallmarks of cancer cells (1). This event emphasizes the importance of maintaining the transcriptional homeostasis in normal cells and places gene expression deregulation at the core of cancer research interests.

46 In the last decades, transcriptomics data derived from cancer specimens has become an important resource for the classification, stratification and molecular driver identification in tumors. We and others 47 48 have demonstrated that deregulation of gene expression is a key node for cancer pathogenesis and progression (2-6). Prostate cancer (PCa) research exemplifies the effort in deciphering the genomics 49 50 and transcriptomics landscape of tumors, and extremely valuable data has been generated (7-13). In spite of the public availability of these relevant data, they are still underexploited by the scientific 51 52 community to understand PCa biology. In this regard, the computational tools and dataset selection strategies to carry out these studies are a bottleneck for the cancer research field. 53

54 By combining integrated-bioinformatics screening of clinically relevant PCa datasets with in vivo and in vitro molecular biology assays, we have recently described the metastasis suppressor activity of 55 Peroxisome proliferator-activated receptor y (PPARy) coactivator alpha (PGC1 α) (14, 15). This 56 57 transcriptional coactivator is a major regulator of mitochondrial biogenesis and function, and has an 58 inherent capacity to integrate environmental signals and cellular energetic demands. This ability empowers PGC1a to be a driver in shaping responses to metabolic stress during different physiologic 59 60 and tumorigenic processes (16). As might be expected due to its fundamental role in normal and cancer scenarios, the regulation of PGC1 α expression, from the genomic to the protein level, is complex and 61 dynamic (17). At the level of mRNA expression, one of the well-defined direct regulators of PGC1ais 62 the Microphthalmia-associated transcription factor (MITF) (18). 63

64 MITF is a basic helix-loop-helix leucine zipper (bHLHZIP) transcription factor that regulates the 65 expression of lineage commitment programs that are essential for propagation of the melanocyte 66 lineage (19). The existence of different MITF transcript variants is the result of both alternative splicing and promoter activation that results in the cell-type-specific expression of the different MITF isoforms 67 (A, CX, MC, C, E, H, D, B, M, J) (20). The melanoma specific isoform M-MITF is the best studied isoform 68 and, despite some controversy, its expression is generally deregulated in melanoma. Although MITF 69 70 alone cannot act as a classical oncogene, it has been called a 'lineage survival oncogene' for melanoma (19, 21). Importantly, the presence or absence of the M-MITF- PGC1a regulatory axis has stratification 71 potential in melanoma and informs on the efficacy of BRAF inhibitor treatments (18, 22). Although the 72 73 expression of MITF has been detected in other types of tumors different from melanoma (23, 24), its active role in the progression of these diseases, including PCa, remains unexplored. 74

Crystallin Alpha-B (CRYAB) is a ubiquitous small heat shock protein that is expressed in response to a wide range of physiological and non-physiological conditions preventing aggregations of denatured proteins. In a wide variety of tumor types CRYAB has been found to be overexpressed and associated with disease progression (25-29) and poor prognosis (30, 31). However, in PCa and nasopharyngeal cancers CRYAB expression is decreased (32, 33), pointing at possible tumor suppressive activity of CRYAB in these cancer scenarios.

In the present study, by combining an exhaustive interrogation of seven publically available prostate cancer databases with refined empirical assays, we have identified MITF as a prostate tumor suppressor. In addition, we have unveiled CRYAB as a novel direct target of the transcription factor that is, at least in part, responsible for its tumor suppressive activity in prostate cancer. Importantly, the tumor suppressive role for this novel MITF-CRYAB axis is supported by the enhanced prognostic potential of a signature based on the concomitant alteration of both genes in PCa patients.

87 **Results**

88 Bioinformatics screening identifies MITF as a transcription factor altered in prostate cancer

We have recently demonstrated that the reduced expression of the transcriptional co-activator PGC1a 89 90 is a causal event for metastatic prostate cancer (PCa) (14). We sought to identify transcriptional 91 regulators related to the alteration in PGC1a expression. We designed a bioinformatics strategy based 92 on the analysis of 16 genes directly linked to the regulation of *PGC1A* gene (17, 22, 34-38), in order to 93 identify transcription factors that could be relevant to PCa biology. For the candidate screen we applied selection criteria based on the consistency of, first, the correlation with PGC1A expression and second, 94 95 the expression of each individual candidate in seven publicly available PCa datasets (7, 9-13) (Figure 1 A). We selected those candidates whose expression in primary tumors correlated with PGC1A (R \geq 96 97 0.2 and p-value \leq 0.05 in more than 50% of the datasets) (Supplementary Figure 1 A) and was altered when compared to normal specimens. For genes exhibiting various transcript variants, the correlation 98 99 analysis was initially performed using the average signal (Supplementary Figure 1 A) and, when available (only Taylor dataset (11)), the correlation was confirmed in all the individual isoforms 100 (Supplementary table 1). The transcription factor MITF was the sole candidate that complied with the 101 established criteria. We observed a consistent correlation between PGC1A and MITF in four out of the 102 103 seven datasets analyzed (Figure 1 B and Supplementary Figure 1 A). In addition, not only the mean expression but also the expression of the individual MITF isoforms were reduced in primary and 104 metastatic PCa specimens when compared with the normal prostate tissue samples (Figure 1 C and 105 Supplementary Figure 1 B). Taken together, our data reveals MITF as a PGC1A-associated 106 107 transcription factor that is consistently downregulated in PCa.

108

109 MITF exhibits tumor suppressive activity in PCa

110 The expression profile of *MITF* in PCa, together with its direct correlation with *PGC1A*, was suggestive 111 of a tumor suppressive activity of the transcription factor. We first examined the differential expression 112 of the distinct mRNA isoforms of *MITF* in normal, PCa primary tumors and PCa cell lines 113 (Supplementary Fig. 2 A-C). *MITFA* was the isoform predominantly expressed in the three scenarios analyzed, and we pursued the studies further with this isoform. Next, we aimed to analyze the biological 114 consequences of ectopic expression of MITFA in PC3 PCa cells. We transduced PC3 cells with a 115 lentiviral vector containing a doxycycline-inducible cassette for the expression of MITFA resulting in the 116 117 generation of the PC3 TRIPZ-MITFA cell line. The induction of MITFA expression (Figure 2 A and B) as well as the regulation of known target genes, including PGC1A (14, 15) (Supplementary Figure 2 D-118 E) was confirmed. We next evaluated the biological outcome of MITFA ectopic expression in PC3 cells 119 and observed that its upregulation significantly reduced two-dimensional and anchorage-independent 120 growth (Figure 2 C and D), with no effect of doxycycline treatment by itself (14). In line with its known 121 function as an inhibitor of cell cycle progression (39), the increased expression of MITFA in PC3 cells 122 resulted in a decrease in BrdU incorporation, a surrogate readout of proliferation (Figure 2 E). 123

In order to ascertain whether the regulation of endogenous *PGC1A* (Supplementary Figure 2 E) was
required for the anti-proliferative effect of MITFA in PC3 cells, we aim at silencing *PGC1A* by using
constitutive (pLKO) expression of short hairpins against it (Supplementary Figure 2 F). Transduction
with the shRNA prevented the upregulation of *PGC1A* upon MITFA induction (Supplementary Figure 2
G) but the anti-proliferative effect of the transcription factor remained unaffected (Supplementary Figure
2 H). These data suggested that the reduced proliferation induced by MITFA was not dependent on the
regulation of endogenous *PGC1A* in PC3 cells.

Importantly, the overall reduction in cell proliferation induced by MITFA was confirmed *in vivo*. Using subcutaneous xenografts assays we observed that MITFA over-expression in PC3 cells (Supplementary Fig. 2 I) led to a marked reduction in the tumor volume (Supplementary Fig. 2 J) and growth rate (Figure 2 F), with no changes in angiogenesis (Supplementary Figure 2 K). Altogether these results demonstrate that MITFA isoform exhibits tumor suppressive activity in PCa.

136

137 Candidate screening of genes mediating the tumor suppressive activity of MITF

138 In order to decipher the molecular mechanism driving the tumor suppressive role of MITFA we 139 performed gene expression profiling of both doxycycline treated and control PC3 TRIPZ-MITFA cells

and identified 101 probes that showed statistically differential signal between both conditions 140 (Supplementary table 2). We first performed a gene enrichment analysis with those genes which 141 displayed upregulated expression (76 genes) upon MITFA over-expression (Figure 3 A and 142 Supplementary table 3), as the number of downregulated genes (25) was no sufficient to obtain any 143 144 gen enrichment. Next, we aimed at identifying potential MITFA effectors of relevance in human PCa. To this end, we established a threshold of 1.5 fold change over MITFA non-induced cells, which resulted 145 in 8 probes (corresponding to 6 annotated genes) upregulated upon the induction of the transcription 146 factor (Supplementary table 2; yellow bold highlighted). We next performed correlation analysis 147 between *MITF* and each of the 6 differentially expressed genes obtained from the microarray (Figure 3 148 A and Supplementary Figure 3 A). The correlation analysis in PCa primary tumor specimens showed 149 that a single gene, Crystallin Alpha B (CRYAB), had a consistent correlation (in more than 50% of 150 151 datasets) with *MITF*, both the mean of isoforms (Figure 3 B and Supplementary Figure 3 A) and the individual isoform A (Supplementary table 4). The MITF-CRYAB correlation was confirmed using an 152 independent cohort of PCa patients from a local hospital (Basurto cohort, Supplementary Figure 3 A). 153 Moreover, the expression of CRYAB either at the level of mRNA (from public datasets and Basurto 154 155 cohort) and protein (from Basurto cohort) was consistently downregulated through the progression of 156 the disease (Figure 3 C and D and Supplementary Figure 3 B-D), supporting the association of MITF and CRYAB expression in PCa. 157

The regulation of CRYAB expression by MITFA was further validated in vitro by western blot and 158 quantitative real-time PCR (gRTPCR) in doxycycline-treated PC3 TRIPZ-MITFA cell lines and in vivo 159 160 by gRTPCR in the xenograft samples (Supplementary Figure 3 E-G). MITF is a transcription factor that regulates gene expression through the DNA binding to E-boxes (Myc-binding sites) (19). In order to 161 confirm the direct regulation of CRYAB expression by MITFA, we screened the promoter of the 162 chaperon and performed chromatin immunoprecipitation assays in two Myc-binding sites (UCSC-163 164 Genome browser; Supplementary Figure 3 H). As predicted, upon doxycycline treatment we detected differential binding of MITFA in both regions of CRYAB promoter (Figure 3 E). 165

Taken together, these data presented *CRYAB* as a direct target of MITFA and the best candidate to
 mediate its tumor suppressive activity in PCa.

168

169 CRYAB mediates the tumor suppressive activity of MITF in PCa

We next studied the functional relevance of CRYAB for the tumor suppressive activity of MITFA in PCa. 170 171 Towards this aim, we constitutively silenced the expression of CRYAB by RNAi using two independent short hairpin RNA (sh#1 and sh#2) in PC3 TRIPZ-MITFA cells. After validation that RNAi was achieved 172 (Figure 4 A and Supplementary Figure 4 A-C) the tumor suppressive activity of MITFA was monitored 173 in control and CRYAB-silenced conditions (PC3 TRIPZ-MITFA scr, sh#1 or sh#2 cell lines). CRYAB 174 silencing blunted the anti-proliferative effects of MITFA in vitro in two-dimensional and anchorage 175 independent growth when compared with scramble shRNA (Figure 4 B and C). Moreover, the reduction 176 in BrdU induced by MITFA was prevented when CRYAB was silenced (Figure 4 D). Importantly, the 177 requirement of CRYAB for the tumor suppressive activity of MITFA was corroborated in vivo (Figure 4 178 179 E and Supplementary Figure 4 D-F). The in vitro and in vivo data demonstrate that the induction of CRYAB is a major effector involved in the tumor suppressive activity of the transcription factor MITF in 180 PCa. 181

We next asked whether the functional association between MITF and CRYAB could be employed to 182 identify PCa patients with high disease aggressiveness. We thus ascertained the stratification potential 183 of the MITF-CRYAB axis in PCa by means of consistency and robustness. We download the mRNA 184 expression raw data together with the clinical data (recurrence or not recurrence) from Taylor (11), 185 Glinsky (8) and TCGA (7) datasets. The individual or average expression signal of CRYAB and MITF 186 genes was calculated for each patient in each dataset. Patients were separated by guartiles according 187 188 to the individual or average signal of CRYAB and MITF genes and then Kaplan-Meyer survival curves were plotted comparing patients with low expression (Quartile 1 - (Q1)) of the individual genes or the 189 gene combination (CRYAB and MITF) versus the rest of the cohort (Q2+Q3+Q4). Strikingly, the 190 signature formed by the average signal of *MITF* and *CRYAB* outperformed the prognostic potential of 191

each individual gene, strongly suggesting that the pathway described herein is strongly associated to
 PCa aggressiveness (Figure 4 F and Supplementary Figure 5).

194 Our data provide solid evidence of an unprecedented MITFA-CRYAB transcriptional axis that exerts 195 tumor suppressive activity in PCa and could positively contribute to disease prognosis.

196

197 DISCUSSION

198 Technological advances in the molecular understanding of cancer have led to a paradigmatic change in the way that we combat the disease. We are now able to deconstruct a tumor at a molecular level 199 200 using genomics, transcriptomics, proteomics and metabolomics. This, in turn, enables us to foresee, identify and demonstrate the potential of patient stratification. Specifically, the transcriptomics 201 202 characterization of tumors is an invaluable strategy to identify clinically relevant genes that play key roles in the progression of cancer, especially for those types with poorer prognosis (14). Thus, the 203 comprehensive and integrative analysis of gene expression changes and clinical parameters in cancer 204 has become a mainstream in cancer research. Mining cancer-associated transcriptome datasets is an 205 emerging approach used by top cancer research groups, but better tools are needed to increase its 206 power and user-friendliness. In order to face this challenge, new interfaces to exploit OMICs data, such 207 as cBioportal (40, 41) are being designed to help scientists interrogate, integrate and visualize large 208 amount of information contained on multiple credible and qualified cancer datasets. 209

In the present study, we exploited publicly available and well-annotated (transcriptomics and clinical data) prostate cancer databases together with experimental assays to describe a novel tumor suppressive activity of the transcription factor MITF in PCa, which is executed, at least in part, through the direct regulation of the CRYAB expression.

The functional implication of MITF in cancer has been best defined in melanoma, in which the expression of the transcription factor is heterogeneous. Although some controversy exists regarding its oncogenic role in melanoma, MITF has been defined as a "lineage survival oncogene" with no data pointing out at a tumor suppressive function (19, 21, 39, 42-45). Even though the expression of MITF

has been detected in other cancer types (23, 24, 46), no data supporting a functional role of MITF
deregulation has been reported yet in a cancer scenario different from melanoma.

Here we show that MITF is downregulated in PCa when compared with normal specimens, in contrast 220 221 to the elevated expression reported in hepatocellular carcinoma (HCC) and chronic myeloid leukemia (CML) (23, 46). Moreover, the novelty of our study relies on the observation and definition of the tumor 222 suppressive activity of MITF in PCa. In this context, MITFA upregulation was associated with a reduction 223 in cell proliferation and DNA replication. As occurs in melanoma, the modulation of MITF expression in 224 PCa cells induces the expression of the cell cycle inhibitor p21 but no changes in the cell cycle inhibitor 225 226 p16 were observed (data not shown). Thus, our results in PCa are in line with the canonical function of MITF in cell cycle progression and proliferation in melanoma (39, 44, 45). 227

It's important to highlight that the tissue specific differences in MITF expression among different cancer
types suggest that in order to fully comprehend MITF's role in cancer, its expression and function has
to be analyzed in context of each particular cell and tissue type.

231 CRYAB is a member of the small heat shock protein family that functions as stress-induced molecular chaperone. It inhibits the aggregation of denatured proteins, promotes cell survival and inhibits 232 apoptosis in the context of cancer (47). Paradoxically, CRYAB is highly expressed in some cancer types 233 234 but decreased in others and in both scenarios an association with cancer progression and prognosis 235 has been reported (25, 26, 28-32, 48-52). In spite of the amount of information regarding the changes in CRYAB expression in cancer, the transcriptional regulation of this chaperone has been poorly 236 explored (48). In this study, we described a novel direct transcriptional regulation of CRYAB by MITF. 237 238 Although there is no direct nor mechanistic evidence of the MITF-CRYAB transcriptional axis in other 239 cancer types, in melanoma both MITF and CRYAB expression are upregulated by BRAF/MEK-inhibitor treatments (49, 52), suggesting that this regulation can go beyond both prostate cancer scenario. 240 Indeed, we observed that the correlation between MITF and CRYAB is also present in colorectal cancer, 241 but not in breast nor lung cancer (data not shown). 242

In our study, the MITF-CRYAB transcriptional axis is reduced and exerts tumor suppressive activity in PCa. This is in agreement with the reduced expression of CRYAB observed in PCa patients and its previous consideration as a protective gene against PCa (32). Yet, the exact molecular mechanism underlying the tumor suppressive activity of CRYAB remains to be elucidated.

Importantly, the extensive interrogation of PCa transcriptomes and associated clinical data has led us to propose the transcriptional axis MITF-CRYAB as a potential prognostic biomarker in PCa. The individual expression of CRYAB and MITF has been previously associated with poor prognosis in various tumor types (26, 29-31, 50, 51) and to therapy response in melanoma (53-55). However, our data showing enhanced prognostic potential of the combined signature provides a new and exciting perspective of the functional interaction of these genes in PCa.

Our study endorses the potential of transcriptional deregulation analysis, as either a cause or a consequence of cancer, and its impact to support the discovery of novel cancer related genes and longterm development of novel cancer treatment strategies.

256 ACKNOWLEDGMENTS

257 Apologies to those whose related publications were not cited due to space limitations. The work of V.Torrano is founded by Fundación Vasca de Innovación e Investigación Sanitarias, BIOEF 258 (BIO15/CA/052), the AECC J.P. Bizkaia and the Basque Department of Health (2016111109). The work 259 of A. Carracedo is supported by the Basque Department of Industry, Tourism and Trade (Etortek) and 260 the department of education (IKERTALDE IT1106-16, also participated by A. Gomez-Muñoz), the BBVA 261 foundation, the MINECO (SAF2016-79381-R (FEDER/EU); Severo Ochoa Excellence Accreditation 262 SEV-2016-0644) and the European Research Council (Starting Grant 336343, PoC 754627). 263 CIBERONC was co-funded with FEDER funds. The work of M. Graupera is supported by the MINECO 264 (SAF2014-59950-P). The work of A. Aransay is supported by the Basque Department of Industry, 265 Tourism and Trade (Etortek and Elkartek Programs), the Innovation Technology Department of Bizkaia 266 County, CIBERehd Network and Spanish MINECO the Severo Ochoa Excellence Accreditation (SEV-267 2016-0644). R. Barrio acknowledges Spanish MINECO (BFU2014-52282-P, Consolider BFU2014-268

57703-REDC), the Departments of Education and Industry of the Basque Government (PI2012/42) and the Bizkaia County. J. Starková acknowledges the Ministry of Health of Czech Republic AZV NV15-28848A. We are thankful to the Basque Biobank for Research (BIOEF) for the custody and management of human prostate specimens used in this study.

273

274 MATERIALS AND METHODS

275 Cell culture and Reagents

Human prostate carcinoma cell lines (PC3) were purchased from Leibniz-Institut DSMZ - Deutsche 276 Sammlung von Mikroorganismen und Zellkulturen GmbH, who provided authentication certificate. The 277 278 cell line used in this study was not found in the database of commonly misidentified cell lines maintained by ICLAC and NCBI Biosample. Cells were transduced with a modified TRIPZ (Dharmacon) doxycycline 279 inducible lentiviral construct in which the RFP and miR30 region was substituted by HA-Flag-MITF. 280 Lentiviral shRNA constructs targeting PGC1A (#1-TRCN0000001165 and #2-TRCN0000001166) and 281 282 CRYAB (#1-TRCN0000010822 and #2-TRCN0000010823) were purchased in Sigma and a scramble 283 shRNA (hairpin sequence: 284 CCGGCAACAAGATGAAGAGCACCAACTCGAGTTGGTGCTCTTCATCTTGTTG) was used as control. For PGC1A and CRYAB shRNAs, Puromycin resistance cassette was replaced by Hygromycin 285 286 cassette from pLKO.1 Hygro (Addgene Ref. 24150) using BamHI and KpnI sites. Cell lines were routinely monitored for mycoplasma contamination and guarantined while treated if positive. 287 Doxycycline hyclate (Dox) and Puromycin were purchased from Sigma, and Hygromycin from 288 Invitrogen. 289

290 Xenotransplant assays

All mouse experiments were carried out following the ethical guidelines established by the Biosafety and Welfare Committee at CIC bioGUNE. The procedures employed were carried out following the recommendations from AAALAC. Xenograft experiments were performed as previously described (14),

injecting 10⁶ cells per condition in two flanks per mouse (Nu/Nu immunodeficient males; 6-12 weeks of
 age). PC3 TRIPZ-HA-MITFA cells alone or under *CRYAB* silencing were injected in each flank of nude
 mice and 24 h post-injections mice were fed with chow or doxycycline diet (Research diets,
 D12100402).

298 Patient samples

All samples were obtained from the Basque Biobank for research (BIOEF, Basurto University hospital) upon informed consent and with evaluation and approval from the corresponding ethics committee (CEIC code OHEUN11-12 and OHEUN14-14).

302 Molecular assays

Western blot was performed as previously described (14). Antibodies used: HA-Tag (Cell Signalling
#3724; dilution 1:10000); MITF (Thermo Fisher Scientific MA5-14146; dilution 1:1000); β-Actin (Cell
Signalling #3700; dilution 1:2000); GAPDH (clone 14C10; Cell Signalling #2218; dilution 1:1000);
CRYAB (Cell Signalling #45844s; dilution 1:1000).

RNA was extracted using NucleoSpin® RNA isolation kit from Macherey-Nagel (ref: 740955.240C). For patients and animal tissues a Trizol-based implementation of the NucleoSpin® RNA isolation kit protocol was used as reported (14). 1µg of total RNA was used for cDNA synthesis using Maxima[™] H Minus cDNA Synthesis Master Mix (Invitrogen M1682). Quantitative Real Time PCR (qRTPCR) was performed as previously described (14). Universal Probe Library (Roche) primers and probes employed are detailed in Supplementary Table 5. *GAPDH* (Hs02758991_g1) housekeeping assay from Applied Biosystems was used for data normalization.

For transcriptomic analysis in PC3 TRIPZ-HA-Flag-MITFA cells, Illumina whole genome -HumanHT-12_V4.0 (DirHyb, nt) method was used as reported (14). A hypergeometric test was used to detect enriched dataset categories.

317 Cellular assays

318 Cell number quantification with crystal violet was performed as referenced (14).

For starvation experiments 100,000 cells per well were seeded in a 6-well plate. Cells were initially plated in 10% FBS media for 24 hours and then the media was changed to FBS free media and left overnight.

Soft agar assays were performed as previously described (14), seeding 5,000 cells per well in 6-well
 plates.

For BrDu incorporation, cells were seeded on glass cover slips in 12-well plates and after 4 days, cells were incubated with 3 μg mL⁻¹ BrDu (Sigma B5002). Cells were fixed with 4% para-formaldehyde, permeabilized with 1% Triton X-100 and incubated with a monoclonal anti-BrDu (MoBU-1) antibody (Invitrogen B35128) at a 1:100 dilution. Images were obtained with an AxioImager D1 microscope (Zeiss). At least three different areas per cover slip were quantified.

329 Chromatin Immunoprecipitation

Chromatin Immunoprecipitation (ChIP) was performed using the SimpleChIP® Enzymatic Chromatin IP 330 Kit (Cat: 9003, Cell Signalling Technology, Inc). Four million PC3 cells were grown in 150 mm dishes 331 either with or without 0.5 μg mL⁻¹ doxycycline during 3 days. Cells from three 150 mm dishes were 332 cross-linked with 35% formaldehyde for 10 min at room temperature. Glycine was added to dishes 333 during 5 min at room temperature. Cells were then washed twice with ice-cold PBS, and scraped into 334 PBS+PMSF. Pelleted cells were lysed and nuclei were harvested following manufacturer's instructions. 335 Nuclear lysates were digested with micrococcal nuclease for 20 min at 37°C and then sonicated in 336 500µl aliquots on ice for 6 pulses of 20 s using a Branson sonicator. Cells were held on ice for at least 337 1 min between sonications. Lysates were clarified at $11,000 \times g$ for 10 min at 4°C, and chromatin was 338 stored at -80°C. HA-Tag polyclonal antibody (Cat: C29F4, Cell Signalling Technology) and IgG antibody 339 (Cat: 2729, Cell Signalling Technology, Inc), were incubated overnight (4°C) with rotation and protein 340 G magnetic beads were incubated 2hrs (4ºC). Washes and elution of chromatin were performed 341 following manufacturer's instructions. DNA quantification was carried out using a Viia7 Real-Time PCR 342 System (Applied Biosystems) with SybrGreen reagents and primers that amplify the predicted MITFA 343 binding region to CRYAB (region 1; For: ttgtttcctcgtagggcttg, Rev: tttcagagccaggagagagc- region 2; 344

For: tctggaatggtgatgtcagg, Rev: attgggtgtggacagaaagc) and *ANGPTL4* (For: gttgacccggctcacaat, Rev:
 ggaacagctcctggcaatc) as a negative binding control.

347 Whole genome gene expression characterization

Whole genome expression characterization was conducted using Human HT12 v4 BeadChips (Illumina Inc.). In brief, cRNA synthesis was obtained with TargetAmp[™] Nano-g[™] Biotin-aRNA Labeling Kit for the Illumina® System, Epicentre (Cat.Num. TAN07924) and subsequent amplification, labeling and hybridization were performed according to Whole-Genome Gene Expression Direct Hybridization Illumina Inc.'s protocol. Raw data were extracted with GenomeStudio analysis software (Illumina Inc.) in the form of GenomeStudio's Final Report (sample probe profile).

354 **Bioinformatic analysis and statistics**

<u>Database normalization:</u> All the datasets used for the data mining analysis were downloaded from GEO and TCGA. GEO-downloaded data was subjected to background correction, log₂ transformation and quartile normalization. In the case of using a pre-processed dataset, this normalization was reviewed and corrected if required. TCGA data were downloaded as upper quartile normalized RSEM count, which was been log2 transformed.

<u>Quartile analysis in Disease Free Survival</u>: Patients biopsies from primary tumours were organized into four quartiles according to the expression of the gene of interest in three datasets. The recurrence of the disease was selected as the event of interest. Kaplan-Meier estimator was used to perform the test as it takes into account *right-censoring*, which occurs if a patient withdraws from a study. On the plot, small vertical tick-marks indicate losses, where a patient's survival time has been right-censored. With this estimator we obtained a survival curve, a graphical representation of the occurrence of the event in the different groups, and a p-value that estimates the statistical power of the differences observed.

367 <u>Correlation analysis</u>: Spearman correlation test was applied to analyse the relationship between paired 368 genes. From this analysis, Spearman coefficient (R) indicates the existing linear correlation 369 (dependence) between two variables *X* and *Y*, giving a value between +1 and -1 (both included), where 1 is total positive correlation, 0 is no correlation, and -1 is total negative correlation. The p-value
indicates the significance of this R coefficient.

Statistical analysis: No statistical method was used to predetermine sample size. The experiments were 372 373 not randomized. The investigators were not blinded to allocation during experiments and outcome assessment. Unless otherwise stated, data analysed by parametric tests is represented by the mean ± 374 s.e.m. of pooled experiments and median ± interguartile range for experiments analysed by non-375 parametric tests. n values represent the number of independent experiments performed, the number of 376 individual mice or patient specimens. For each independent *in vitro* experiment, at least two technical 377 378 replicates were used and a minimum number of three experiments were done to ensure adequate statistical power. For data mining analysis, ANOVA test was used for multi-component comparisons 379 and Student T test for two component comparisons. In the *in vitro* experiments, normal distribution was 380 confirmed or assumed (for n<5) and Student T test was applied for two component comparisons. In the 381 382 statistical analyses involving fold changes, one sample t-test with a hypothetical value of 1 was performed. The confidence level used for all the statistical analyses was of 95% (alpha value = 0.05). 383 Two-tail statistical analysis was applied for experimental design without predicted result, and one-tail 384 for validation or hypothesis-driven experiments. 385

386 <u>Gene expression array data analysis:</u> first, raw expression data were background-corrected, log2-387 transformed and quantile-normalized using the lumi R package7

, available through the Bioconductor repository. Probes with a "detection p-value" lower than 0.01 in at
least one sample were considered expressed. For the detection of differentially expressed genes, a
linear model was fitted to the probe data and empirical Bayes moderated t-statistics were calculated
using the limma package from Bioconductor. Only genes with differential fold-change (FC) >1.5 or <-
1.5 and an adjusted p-value < 0.05 were considered as differentially expressed.

393 Accession numbers and datasets

- Primary accessions: The transcriptomic data generated in this publication have been deposited in NCBI's Gene Expression Omnibus and are accessible through GEO Series accession number GSE114345 (https://www.ncbi.nlm.nih.gov/geo/query/acc.cgi?acc=GSE114345).
- 397 Referenced accessions: TCGA <u>https://cancergenome.nih.gov/</u>, Grasso *et* al., GEO: GSE35988 (9);
- Lapointe et al., GEO: GSE3933 (10); Taylor et al., GEO: GSE21032 (11); Tomlins et al., GEO:
- 399 GSE6099 (12); Varambally *et* al., GEO: GSE3325 (13); and Glinsky et al (8).

400 AUTHOR CONTRIBUTIONS

401 LV-J and AM performed the majority of in vitro and in vivo experiments, unless specified otherwise. NM-M contributed to the in vivo experiments, experimental design and 402 403 discussion. ARC carried out the bioinformatics and biostatistical analysis. AS-C, MP-V, 404 IH and IA contributed to in vitro analysis and provided technical support. IL-V, AS-M, AL-I and MU-U provided BPH and PCa samples for gene expression analysis from Basurto 405 406 University Hospital. MGr carried out microvessel staining and quantifications. JS contributed as supervisor of IH. JDS and RB performed or coordinated (RB) the cloning 407 408 of *MITFA* in lentiviral vectors. AMMA contributed to experimental design and discussion. 409 AC contributed to experimental design, data analysis and discussion. VT supervised the project, contributed to the experimental design, data generation, analysis and discussion 410 and wrote the manuscript. 411

413 **REFERENCES**

414 1. Hanahan D, Weinberg RA. Hallmarks of cancer: the next generation. Cell.415 2011;144(5):646-74.

416 2. Martin-Martin N, Carracedo A, Torrano V. Metabolism and Transcription in Cancer:
417 Merging Two Classic Tales. Front Cell Dev Biol. 2017;5:119.

418 3. Martin-Martin N, Piva M, Urosevic J, Aldaz P, Sutherland JD, Fernandez-Ruiz S, et al.
419 Stratification and therapeutic potential of PML in metastatic breast cancer. Nat Commun.
420 2016;7:12595.

Martin-Martin N, Zabala-Letona A, Fernandez-Ruiz S, Arreal L, Camacho L, Castillo Martin M, et al. PPARdelta Elicits Ligand-Independent Repression of Trefoil Factor Family to Limit
 Prostate Cancer Growth. Cancer Res. 2018;78(2):399-409.

Bacolod MD, Das SK, Sokhi UK, Bradley S, Fenstermacher DA, Pellecchia M, et al.
Examination of Epigenetic and other Molecular Factors Associated with mda-9/Syntenin
Dysregulation in Cancer Through Integrated Analyses of Public Genomic Datasets. Adv Cancer
Res. 2015;127:49-121.

6. Olvedy M, Tisserand JC, Luciani F, Boeckx B, Wouters J, Lopez S, et al. Comparative
oncogenomics identifies tyrosine kinase FES as a tumor suppressor in melanoma. J Clin Invest.
2017;127(6):2310-25.

431 7. Cancer Genome Atlas Research N. The Molecular Taxonomy of Primary Prostate Cancer.
432 Cell. 2015;163(4):1011-25.

433 8. Glinsky GV, Glinskii AB, Stephenson AJ, Hoffman RM, Gerald WL. Gene expression
434 profiling predicts clinical outcome of prostate cancer. J Clin Invest. 2004;113(6):913-23.

435 9. Grasso CS, Wu YM, Robinson DR, Cao X, Dhanasekaran SM, Khan AP, et al. The
436 mutational landscape of lethal castration-resistant prostate cancer. Nature.
437 2012;487(7406):239-43.

438 10. Lapointe J, Li C, Giacomini CP, Salari K, Huang S, Wang P, et al. Genomic profiling reveals
439 alternative genetic pathways of prostate tumorigenesis. Cancer Res. 2007;67(18):8504-10.

Taylor BS, Schultz N, Hieronymus H, Gopalan A, Xiao Y, Carver BS, et al. Integrative
genomic profiling of human prostate cancer. Cancer Cell. 2010;18(1):11-22.

Tomlins SA, Mehra R, Rhodes DR, Cao X, Wang L, Dhanasekaran SM, et al. Integrative
molecular concept modeling of prostate cancer progression. Nat Genet. 2007;39(1):41-51.

444 13. Varambally S, Yu J, Laxman B, Rhodes DR, Mehra R, Tomlins SA, et al. Integrative genomic
445 and proteomic analysis of prostate cancer reveals signatures of metastatic progression. Cancer
446 Cell. 2005;8(5):393-406.

Torrano V, Valcarcel-Jimenez L, Cortazar AR, Liu X, Urosevic J, Castillo-Martin M, et al.
The metabolic co-regulator PGC1alpha suppresses prostate cancer metastasis. Nat Cell Biol.
2016;18(6):645-56.

450 15. Valcarcel-Jimenez L, Torrano V, Carracedo A. New insights on prostate cancer 451 progression. Cell Cycle. 2017;16(1):13-4.

452 16. Valcarcel-Jimenez L, Gaude E, Torrano V, Frezza C, Carracedo A. Mitochondrial
453 Metabolism: Yin and Yang for Tumor Progression. Trends Endocrinol Metab. 2017;28(10):748454 57.

455 17. Hock MB, Kralli A. Transcriptional control of mitochondrial biogenesis and function.456 Annu Rev Physiol. 2009;71:177-203.

Haq R, Shoag J, Andreu-Perez P, Yokoyama S, Edelman H, Rowe GC, et al. Oncogenic
BRAF regulates oxidative metabolism via PGC1alpha and MITF. Cancer Cell. 2013;23(3):302-15.

459 19. Wellbrock C, Arozarena I. Microphthalmia-associated transcription factor in melanoma
460 development and MAP-kinase pathway targeted therapy. Pigment Cell Melanoma Res.
461 2015;28(4):390-406.

462 20. Tachibana M. MITF: a stream flowing for pigment cells. Pigment Cell Res. 463 2000;13(4):230-40.

Garraway LA, Widlund HR, Rubin MA, Getz G, Berger AJ, Ramaswamy S, et al. Integrative
genomic analyses identify MITF as a lineage survival oncogene amplified in malignant
melanoma. Nature. 2005;436(7047):117-22.

467 22. Vazquez F, Lim JH, Chim H, Bhalla K, Girnun G, Pierce K, et al. PGC1alpha expression 468 defines a subset of human melanoma tumors with increased mitochondrial capacity and 469 resistance to oxidative stress. Cancer Cell. 2013;23(3):287-301.

470 23. Aggoune D, Sorel N, Bonnet ML, Goujon JM, Tarte K, Herault O, et al. Bone marrow
471 mesenchymal stromal cell (MSC) gene profiling in chronic myeloid leukemia (CML) patients at
472 diagnosis and in deep molecular response induced by tyrosine kinase inhibitors (TKIs). Leuk Res.
473 2017;60:94-102.

474 24. Li Y, Kong D, Ahmad A, Bao B, Sarkar FH. Targeting bone remodeling by isoflavone and
475 3,3'-diindolylmethane in the context of prostate cancer bone metastasis. PLoS One.
476 2012;7(3):e33011.

477 25. Moyano JV, Evans JR, Chen F, Lu M, Werner ME, Yehiely F, et al. AlphaB-crystallin is a
478 novel oncoprotein that predicts poor clinical outcome in breast cancer. J Clin Invest.
479 2006;116(1):261-70.

480 26. Voduc KD, Nielsen TO, Perou CM, Harrell JC, Fan C, Kennecke H, et al. alphaB-crystallin
481 Expression in Breast Cancer is Associated with Brain Metastasis. NPJ Breast Cancer. 2015;1.

482 27. Shi C, Yang X, Bu X, Hou N, Chen P. Alpha B-crystallin promotes the invasion and 483 metastasis of colorectal cancer via epithelial-mesenchymal transition. Biochem Biophys Res 484 Commun. 2017;489(4):369-74.

Yilmaz M, Karatas OF, Yuceturk B, Dag H, Yener M, Ozen M. Alpha-B-crystallin expression
in human laryngeal squamous cell carcinoma tissues. Head Neck. 2015;37(9):1344-8.

Volkmann J, Reuning U, Rudelius M, Hafner N, Schuster T, Becker VRA, et al. High
expression of crystallin alphaB represents an independent molecular marker for unfavourable
ovarian cancer patient outcome and impairs TRAIL- and cisplatin-induced apoptosis in human
ovarian cancer cells. Int J Cancer. 2013;132(12):2820-32.

491 30. Qin H, Ni Y, Tong J, Zhao J, Zhou X, Cai W, et al. Elevated expression of CRYAB predicts
492 unfavorable prognosis in non-small cell lung cancer. Med Oncol. 2014;31(8):142.

493 31. Shi C, He Z, Hou N, Ni Y, Xiong L, Chen P. Alpha B-crystallin correlates with poor survival
494 in colorectal cancer. Int J Clin Exp Pathol. 2014;7(9):6056-63.

495 32. Altintas DM, Allioli N, Decaussin M, de Bernard S, Ruffion A, Samarut J, et al.
496 Differentially expressed androgen-regulated genes in androgen-sensitive tissues reveal
497 potential biomarkers of early prostate cancer. PLoS One. 2013;8(6):e66278.

498 33. Huang Z, Cheng Y, Chiu PM, Cheung FM, Nicholls JM, Kwong DL, et al. Tumor suppressor
499 Alpha B-crystallin (CRYAB) associates with the cadherin/catenin adherens junction and impairs
500 NPC progression-associated properties. Oncogene. 2012;31(32):3709-20.

501 34. Borniquel S, Garcia-Quintans N, Valle I, Olmos Y, Wild B, Martinez-Granero F, et al. 502 Inactivation of Foxo3a and subsequent downregulation of PGC-1 alpha mediate nitric oxide-503 induced endothelial cell migration. Mol Cell Biol. 2010;30(16):4035-44.

504 35. Jin J, Iakova P, Jiang Y, Lewis K, Sullivan E, Jawanmardi N, et al. Transcriptional and 505 translational regulation of C/EBPbeta-HDAC1 protein complexes controls different levels of p53, 506 SIRT1, and PGC1alpha proteins at the early and late stages of liver cancer. J Biol Chem. 507 2013;288(20):14451-62.

Sancho P, Burgos-Ramos E, Tavera A, Bou Kheir T, Jagust P, Schoenhals M, et al.
MYC/PGC-1alpha Balance Determines the Metabolic Phenotype and Plasticity of Pancreatic
Cancer Stem Cells. Cell Metab. 2015;22(4):590-605.

511 37. Shimizu YI, Morita M, Ohmi A, Aoyagi S, Ebihara H, Tonaki D, et al. Fasting induced up-512 regulation of activating transcription factor 5 in mouse liver. Life Sci. 2009;84(25-26):894-902. 513 38. Wende AR, O'Neill BT, Bugger H, Riehle C, Tuinei J, Buchanan J, et al. Enhanced cardiac 514 Akt/protein kinase B signaling contributes to pathological cardiac hypertrophy in part by 515 impairing mitochondrial function via transcriptional repression of mitochondrion-targeted 516 nuclear genes. Mol Cell Biol. 2015;35(5):831-46.

S17 39. Carreira S, Goodall J, Aksan I, La Rocca SA, Galibert MD, Denat L, et al. Mitf cooperates
with Rb1 and activates p21Cip1 expression to regulate cell cycle progression. Nature.
2005;433(7027):764-9.

40. Cerami E, Gao J, Dogrusoz U, Gross BE, Sumer SO, Aksoy BA, et al. The cBio cancer
genomics portal: an open platform for exploring multidimensional cancer genomics data. Cancer
Discov. 2012;2(5):401-4.

41. Gao J, Aksoy BA, Dogrusoz U, Dresdner G, Gross B, Sumer SO, et al. Integrative analysis
of complex cancer genomics and clinical profiles using the cBioPortal. Sci Signal. 2013;6(269):pl1.
42. Carreira S, Goodall J, Denat L, Rodriguez M, Nuciforo P, Hoek KS, et al. Mitf regulation of

526 Dia1 controls melanoma proliferation and invasiveness. Genes Dev. 2006;20(24):3426-39.

527 43. Vachtenheim J, Ondrusova L. Microphthalmia-associated transcription factor expression
528 levels in melanoma cells contribute to cell invasion and proliferation. Exp Dermatol.
529 2015;24(7):481-4.

530 44. Wellbrock C, Marais R. Elevated expression of MITF counteracts B-RAF-stimulated 531 melanocyte and melanoma cell proliferation. J Cell Biol. 2005;170(5):703-8.

45. Wellbrock C, Rana S, Paterson H, Pickersgill H, Brummelkamp T, Marais R. Oncogenic
BRAF regulates melanoma proliferation through the lineage specific factor MITF. PLoS One.
2008;3(7):e2734.

535 46. Thomaschewski M, Riecken K, Unrau L, Volz T, Cornils K, Ittrich H, et al. Multi-color RGB
536 marking enables clonality assessment of liver tumors in a murine xenograft model. Oncotarget.
537 2017;8(70):115582-95.

Kamradt MC, Lu M, Werner ME, Kwan T, Chen F, Strohecker A, et al. The small heat shock
protein alpha B-crystallin is a novel inhibitor of TRAIL-induced apoptosis that suppresses the
activation of caspase-3. J Biol Chem. 2005;280(12):11059-66.

541 48. Zhang L, Zhang L, Xia X, He S, He H, Zhao W. Kruppel-like factor 4 promotes human
542 osteosarcoma growth and metastasis via regulating CRYAB expression. Oncotarget.
543 2016;7(21):30990-1000.

Hu R, Aplin AE. alphaB-crystallin is mutant B-RAF regulated and contributes to cyclin D1
turnover in melanocytic cells. Pigment Cell Melanoma Res. 2010;23(2):201-9.

546 50. Chin D, Boyle GM, Williams RM, Ferguson K, Pandeya N, Pedley J, et al. Alpha B-crystallin,
547 a new independent marker for poor prognosis in head and neck cancer. Laryngoscope.
548 2005;115(7):1239-42.

549 51. Shi QM, Luo J, Wu K, Yin M, Gu YR, Cheng XG. High level of alphaB-crystallin contributes 550 to the progression of osteosarcoma. Oncotarget. 2016;7(8):9007-16.

52. Smith MP, Brunton H, Rowling EJ, Ferguson J, Arozarena I, Miskolczi Z, et al. Inhibiting
Drivers of Non-mutational Drug Tolerance Is a Salvage Strategy for Targeted Melanoma Therapy.
Cancer Cell. 2016;29(3):270-84.

53. Muller J, Krijgsman O, Tsoi J, Robert L, Hugo W, Song C, et al. Low MITF/AXL ratio predicts early resistance to multiple targeted drugs in melanoma. Nat Commun. 2014;5:5712.

556 54. Naffouje S, Naffouje R, Bhagwandin S, Salti GI. Microphthalmia transcription factor in 557 malignant melanoma predicts occult sentinel lymph node metastases and survival. Melanoma 558 Res. 2015;25(6):496-502.

559 55. Najem A, Krayem M, Sales F, Hussein N, Badran B, Robert C, et al. P53 and MITF/Bcl-2 560 identified as key pathways in the acquired resistance of NRAS-mutant melanoma to MEK 561 inhibition. Eur J Cancer. 2017;83:154-65.

564 Figure legends

565 Figure 1. MITF expression correlates with PGC1A expression and is 566 downregulated in PCa. A. Schematic representation of candidate screening to mediate PGC1A downregulation in PCa. Candidate selection was performed by applying two 567 568 different selection criteria based on the consistency within the datasets used (>50%); the 569 expression of the candidate must be consistently (i) correlated with the PGC1A's and (ii) 570 altered in the disease. B. Correlation analysis between PGC1A and MITF expression in 571 primary tumor (PT) specimens of different PCa datasets ((9-11) and TCGA provisional). 572 Sample sizes: Grasso n=45; Lapointe n=13; Taylor n=131 and TCGA provisional n=495. 573 **C.** MITF expression in normal prostate and primary tumors (PT) specimens in different 574 data sets (9-11). Correlation (B) and expression (C) data from Taylor dataset 575 corresponds to the mean signal of all isoforms of the transcripts. In B and C, each dot corresponds to an individual specimen. Sample sizes: Grasso et al. (Normal, n=12; PT, 576 n=45); Lapointe et al. (Normal, n=9; PT, n=13); Taylor et al. (Normal, n=29; PT, n=131). 577 578 Error bars represent s.e.m. Statistic test: Spearman correlation R (B) and Mann Whitney 579 test (C). p, p-value.

Figure 2. MITF exhibits tumor suppressive activity in PC3 PCa cell line. A-B. 580 581 Analysis and quantification of MITF expression by qRTPCR (A, n=8)) and western blot 582 (B, representative experiment out of 3 independent ones) in PC3 TRIPZ-MITFA cells 583 after treatment with 0.5 µg mL⁻¹ doxycycline (Dox). C. Relative cell number quantification 584 by crystal violet in doxycycline treated and non-treated PC3 TRIPZ-MITFA cells. Data is 585 normalized to day 0. Asterisks indicate statistics of 5 independent experiments. One 586 representative experiment out of 5 is shown. Error bars represent standard deviation. D-587 E. Effect of MITF induction on anchorage independent growth (D, soft agar; n=4 independent experiments) and BrdU incorporation (E, n=3 independent experiments). F. 588 Impact of MITF induction in tumor growth rate of PC3 TRIPZ-MITFA cells (n=7 animals 589 per group; 14 injections/tumors). No dox: MITFA non-induced conditions; Dox: MITFA 590

induced conditions. Error bars represent s.e.m (A, D and E) or minimun and maximum
values (H). Statistic test: One sample t-test (A, D and E) and Student t-test (C and F. *p
< 0.05, **p < 0.01, ***p < 0.001.

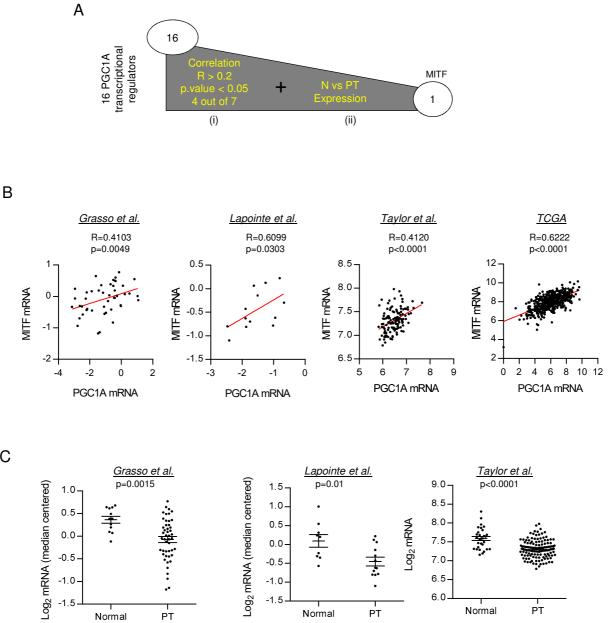
594 Figure 3. CRYAB is the candidate to mediate its tumor suppressive activity in PCa.

A. Workflow of the candidate screening. B. Correlation analysis between MITF and 595 596 CRYAB expression in primary tumor (PT) specimens of different PCa datasets. Sample 597 sizes: Taylor, n=131; Grasso, n=49; Lapointe, n=13; TCGA provisional data, n=495; and 598 Glinsky, n=78. C. CRYAB expression in normal prostate and primary tumor (PT) 599 specimens in different PCa datasets (9-13). Sample sizes: Taylor (N, n=29; PT, n=130); 600 Grasso (N, n=12; PT, n=49); Varambally (N, n=6; PT, n=7); Lapointe et al. (N, n=9; PT, 601 n=13) and Tomlins (N, n=22; PT, n=32). Data from Taylor dataset corresponds to the 602 mean signal of all isoforms of the transcripts. In B and C, each dot corresponds to an 603 individual specimen. D. Western blot analysis of CRYAB expression in benign prostatic 604 hyperplasia (BPH) and PCa specimens from Basurto University Hospital cohort (BPH 605 specimens; n=7 patient PCa n=14 patient specimens). Ε. Chromatin immunoprecipitation (ChIP) of exogenous MITF on CRYAB promoter in PC3 TRIPZ-606 607 MITFA cells after induction with 0.5 µg mL-1 doxycycline for 3 days (n=4-5). Binding to ANGPT4 was used as a negative control. Final data was normalized to IgG (negative-608 609 immunoprecipitation control) and to No dox condition. No dox: MITFA non-induced 610 conditions; Dox: MITFA induced conditions. Statistic tests: Spearman correlation (B); 611 Mann Whitney test (C); one sample t test (E); Error bars represent s.e.m. *p < 0.05, **p612 < 0.01.

Figure 4. CRYAB mediates the tumor suppressor activity of MITF. A. Analysis of MITFA and CRYAB protein expression in doxycycline-treated PC3 TRIPZ-MITFA cells transduced with shScramble (scr) or two independent shCRYAB (sh#1 and#2) (one representative experiment with technical duplicates is shown; similar results were obtained in three independent experiments). **B**. Relative cell number quantification by

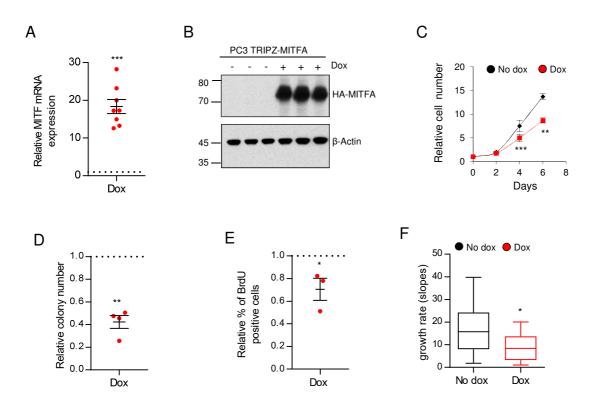
618 crystal violet in doxycycline-treated and non-treated PC3 TRIPZ-MITFA cells, in the 619 presence (scr) or absence (sh#1, 2) of CRYAB (n=5 independent experiments). Data is 620 normalized to day 0 and represented as cell number at day 6 relative to No Dox condition 621 (depicted by a dotted line). C-D. Effect of CRYAB silencing on anchorage independent 622 growth (C, soft agar; n=4 independent experiments) and BrdU incorporation (D, n=3 623 independent experiments) in PC3 TRIPZ-MITFA cells after treatment with 0.5 µg mL⁻¹ 624 doxycycline. E. Impact of CRYAB silencing in tumor growth rate of MITF-induced cells 625 (n=10 animals per group-scr or sh#1; 2 injections per mice; (scr No dox, n=10 tumors; 626 sh#1 No dox, n=8 tumors; scr Dox, n=6 tumors; sh#1 Dox, n=11 tumors). F. Association 627 of the mean signal of MITF and CRYAB with disease-free survival (DFS) in three PCa 628 data sets (Q1: first quartile distribution; rest: second, third and fourth quartile distribution. Sample sizes: Taylor, primary tumors n=131; TCGA provisional data primary tumors 629 630 n=490; Glinsky, primary tumors n=78. No dox: MITFA non-induced conditions; Dox: 631 MITFA induced conditions. HR: Hazard Ratio. Statistic tests: One sample t test (B, C and 632 D – No dox vs Dox conditions); Unpaired Student t-test (t) (B, C and D – Dox-treated scr 633 vs Dox-treated sh#1/2); Log-rank (Mantel-Cox) test (F). Error bars represent s.e.m. */\$ 634 p < 0.05, **/\$\$p < 0.01. Asterisks indicate statistic between No dox and Dox conditions 635 and dollar symbol between Dox-treated scr and Dox-treated sh#1 or 2.

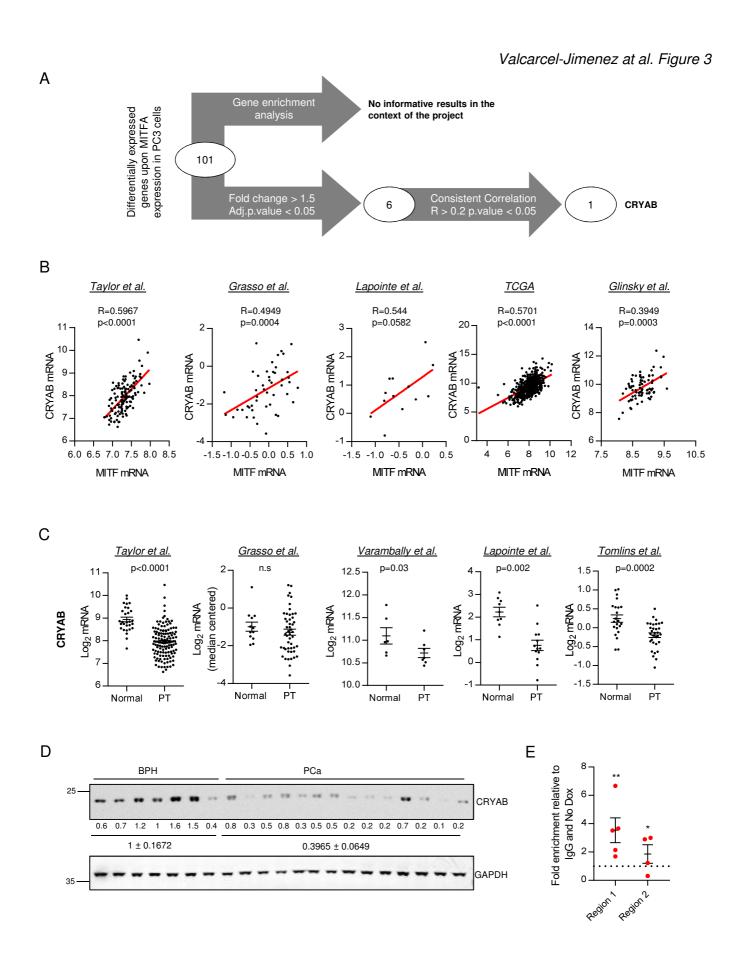
Valcarcel-Jimenez at al. Figure 1



С

Valcarcel-Jimenez at al. Figure 2





Valcarcel-Jimenez at al. Figure 4

